https://doi.org/10.1093/nargab/lqac078

PDBspheres: a method for finding 3D similarities in local regions in proteins

Adam T. Zemla[1,*], Jonathan E. Allen[1], Dan Kirshner[2] and Felice C. Lightstone[2]

[1]Global Security Computing Applications, Lawrence Livermore National Laboratory, Livermore, CA 94550, USA and [2]Biosciences and Biotechnology Division, Physical and Life Sciences Directorate, Lawrence Livermore National Laboratory, Livermore, CA 94550, USA

Received January 27, 2022; Revised August 06, 2022; Editorial Decision September 26, 2022; Accepted September 29, 2022

ABSTRACT

We present a structure-based method for finding and evaluating structural similarities in protein regions relevant to ligand binding. PDBspheres comprises an exhaustive library of protein structure regions ('spheres') adjacent to complexed ligands derived from the Protein Data Bank (PDB), along with methods to find and evaluate structural matches between a protein of interest and spheres in the library. PDBspheres uses the LGA (Local–Global Alignment) structure alignment algorithm as the main engine for detecting structural similarities between the protein of interest and template spheres from the library, which currently contains >2 million spheres. To assess confidence in structural matches, an all-atom-based similarity metric takes side chain placement into account. Here, we describe the PDBspheres method, demonstrate its ability to detect and characterize binding sites in protein structures, show how PDBspheres—a strictly structure-based method—performs on a curated dataset of 2528 ligand-bound and ligand-free crystal structures, and use PDBspheres to cluster pockets and assess structural similarities among protein binding sites of 4876 structures in the 'refined set' of the PDBbind 2019 dataset.

INTRODUCTION

Interactions between proteins and small-molecule ligands are a cornerstone of biochemical function. Modern drug discovery often relies on structural information about the target of interest (typically a protein). However, when a new structure is obtained, it may be the case that little is known with regard to potential binding sites on that structure. Numerous studies have focused on understanding protein–ligand interactions [e.g. (1,2)] to further the development of binding site prediction methods [e.g. (3–6)] as well as benchmark datasets [e.g. (7–11)] used to compare and evaluate their performance. In general, the binding site prediction methods can be categorized into three broad sets: (i) template-based methods that use known protein information; (ii) physics-based methods that rely on geometry (e.g. cavity detection) and/or physicochemical properties (e.g. surface energy interactions with probe molecules); and (iii) machine learning (ML)—rapidly developing in recent years—methods capable of efficiently processing information collected in their training datasets. For ML methods, data can come from both experiments and *in silico* data processing, as described, for example, in (12–15). Our method, PDBspheres, is template based; however, it relies solely on local structure conformation similarities with templates extracted from structures from the Protein Data Bank (PDB)—i.e. PDBspheres does not use any prior information from libraries of sequences, motifs or residues forming binding sites that are collected separately to enhance the method performance. In general, template-based methods can be categorized as (i) those that rely on only protein sequence, e.g. Firestar (16), (ii) those that rely on only protein structure, e.g. SP-ALIGN (17), or (iii) those that rely on both sequence and structure, e.g. Concavity (18). Some methods, e.g. SURFNET (19), are classified as structure-based methods, but since they use geometric characteristics, they are grouped within geometry-based methods (20).

One of the strengths of the developed PDBspheres method is that in the binding site searches we use only those template models of cavities (PDBspheres library) that are already observed as protein–ligand binding sites in other proteins (experimentally solved protein–ligand complexes deposited in the PDB). This approach ensures that any structural shape that might resemble a cavity in evaluated protein models—e.g. holes within interchain interfaces, missing fragments in coordinates or other structural imperfections in geometry—will not be reported by PDBspheres searches as cavity candidates, simply because they are not evidenced as *ligand-binding* cavities in reality, i.e. in confirmed-by-experiment PDB structures. To resolve the problem with this kind of false-positive pocket assignments,

[*]To whom correspondence should be addressed. Tel: +1 925 423 5571; Fax: +1 925 423 6437; Email: zemla1@llnl.gov

some template-based methods may need additional information about proteins collected from calculated sequence alignments, patterns in residues forming binding sites, etc. A natural strength of structure template-based methods such as PDBspheres lies in their ability to detect similar binding sites and help determine the biochemical function even if the sequence identity is very low, i.e. when similarity between pockets cannot be detected with confidence based on the sequence. A limitation, however, of the PDBspheres method is that its library depends on structural information derived from the PDB database, so identification of a new pocket or function relies on data availability in the PDB, i.e. pockets having shapes not represented in the PDB will not be found.

In the PDBspheres method, binding sites are identified exclusively based on the structure similarity between regions from the query protein and pocket spheres from the PDBspheres library. Ligand placement within a predicted pocket is calculated based on a protein–sphere superposition, i.e. an agreement in structure conformation between atoms from the query protein and protein atom coordinates from the template sphere. The main premise of structure template-based binding site prediction methods is that the number of pockets is limited (2); therefore, each one of them may serve as a binding site for a large diversity of ligands (17). However, possible conformations of ligands bound in the pocket are also limited. Indeed, when we predict a ligand–protein conformation, we focus on what parts of the ligand (e.g. its core region) need to be in a correct conformation, i.e. a conformation that can be confirmed by experiment and from which the binding affinities can be estimated. Usually such 'correct' conformations are shared between ligands that bind a given pocket (at least shared by their 'core' regions). The evaluation of the correctness of the ligand placement within a pocket is not an easy task. For example, when for a given protein two pocket predictions with different ligands inserted need to be evaluated, a simple calculation and comparison of the ligand centroids (the center of mass of the bound ligands) can be misleading. This is because the two predictions may differ in assigned placements of the ligands within a pocket (especially when the pocket size is large allowing the ligands to fit in different areas within the cavity), or the ligand sizes and their shapes are different [e.g. some parts of the ligands can be exposed outside the pocket with different orientations (21); see Figure 1]. These difficulties in the assessment of the accuracy of binding site predictions and ligand placements within predicted pockets could be overcome when we focus on the evaluation of residues interacting with the bound ligands. In Figure 1, we present an example of the b1 domain from the human neuropilin-1 (PDB 2qqi) where two different poses of the same ligand EG01377 (PDB ID: DUE) are possible (21). Superposition of two experimentally solved structures of neuropilin-1 b1 domain in complex with EG01377 shows almost identical protein structure conformations, while poses of bound ligands differ significantly outside the 'core'. The distance between centroids of the ligand's two orientations placed in the pocket is >4.6 Å when the centroid is calculated on all ligand's atoms, and only 0.7 Å when it is calculated on the buried parts of the ligand—'core'.

Knowing the correct 'core' conformation of the ligand within the pocket (i.e. the pose of the conserved part) can significantly improve '*in silico*' drug discovery; it can be used in compound screening/docking efforts as a pre-filter for selection of most promising compounds for a more detailed and expensive computational evaluation. Currently, there are millions of compounds screened using docking or molecular mechanics-generalized Born surface area approaches. These methods are widely used to estimate ligand-binding affinities in identified binding sites of targeted proteins to find good candidates for a further (experimental) analysis of potential inhibitors.

Assessment of the performance of binding site prediction methods is not an easy task because they may perform differently on different benchmarks. In Critical Assessment of Protein Structure Prediction (CASP) experiments (rounds 8, 9 and 10) (22–24), an attempt was made to compare different ligand binding residue prediction methods, but it was found that the assessment might be biased (not enough targets, targets not diverse enough to represent different families, folds, ligand type and ligand binding sites) and this category was subsequently dropped from CASP. A comprehensive benchmark dataset was recently designed by Clark *et al.* (25,26). It covers 304 unique protein families with 2528 structures in 1456 'holo' and 1082 'apo' conformations. A detailed comparison analysis using this benchmark dataset was performed on seven binding site prediction methods (25). The authors decided to exclude template-based methods from their evaluation to avoid unfair comparison with non-template-based methods. As stated in (25), template-based methods use 'libraries of sequence-based template information', which 'would inevitably lead to the use of holo structure knowledge to solve the binding site locations in apo structures'. So, it was expected that template-based methods would easily outperform non-template-based methods on the benchmark. The accuracy of pocket prediction methods in Clark *et al.*'s (25) analysis and during CASP was measured mainly by the Matthew's correlation coefficient (MCC). This metric assigns high scores not just when at least one residue in a given binding site is identified correctly, but rather rewards methods with more correct and less false predictions of contact residues implying which of the algorithm pocket predictions are close to the 'correct' location on the binding surface of the protein. In this paper, we use the same metric to evaluate the performance of our method with varying datasets of structural templates used by PDBspheres to make predictions. Our reported results were merged with results from the assessment of non-template-based methods performed by Clark *et al.* (25) in Table 1 and also a discussion of the performance of template-based methods from CASP (22–24) is included to illustrate how PDBspheres places within these methods and what the limits of structure-based pocket prediction methods may be.

MATERIALS AND METHODS

The PDBspheres system is designed to help assess the similarity between proteins based on their structure similarity in selected local regions (e.g. binding sites, protein interfaces or any other local regions that might be structurally charac-

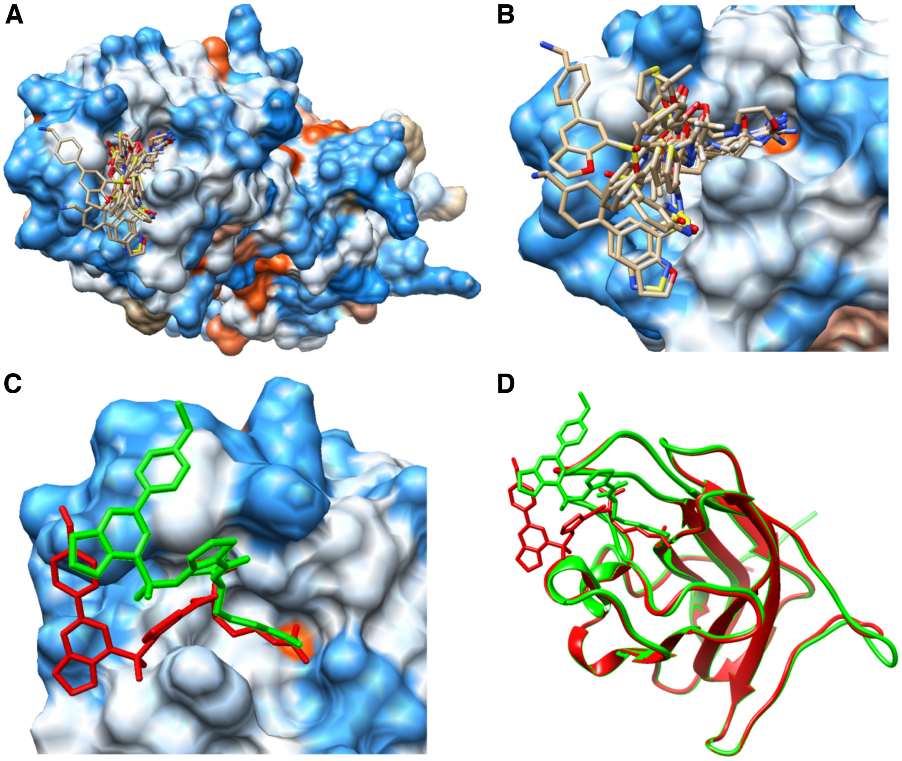

Figure 1. (**A**) Example of the b1 domain from the human neuropilin-1 (PDB 2qqi) where a single pocket can serve as a binding site for many different ligands. (**B**) Zoom-in to the pocket that can accommodate ligands of different sizes. A list of ligands includes 6JY.20 (Arg-7), 6K8.24 (Arg-6), 8DR.32 (EG00229), AAG.15 (M45), AR5.19 (Arg-5), BCN.23 (bicine), DUE.40 (EG01377), HRG.13 (Arg-1) and R40.22 (Arg-4), where ligand information 'PDBid.size' is provided with a size representing a number of heavy atoms. (**C**) Two different poses of the ligand DUE.40 (EG01377) are reported in (21) and identified by PDBspheres based on two templates: 6fmc and 6fmf. (**D**) Superposition of two experimentally solved structures of neuropilin-1 b1 domain in complex with EG01377 (in green: PDB 6fmc at resolution of 0.9 Å; in red: PDB 6fmf at resolution of 2.8 Å) shows almost identical protein structure conformations, while poses of bound ligands differ significantly outside the core. The distance between centroids of the ligand's two orientations when placed in the pocket is >4.6 Å.

teristic of a particular group of proteins). The PDBspheres system has three main components: (i) the PDBspheres library of binding site templates; (ii) a structure similarity search algorithm to detect similarity between evaluated local structural regions (e.g. binding sites); and (iii) numerical metrics to assess confidence in detected similar regions.

Currently, the PDBspheres library (ver. 2021/10/13) contains 2 002 354 compound binding site models (template spheres) and 67 445 short-peptide binding site models derived from protein structures deposited in the PDB database (27).

The Local–Global Alignment (LGA) program (28) is used to perform all structure similarity searches. While comparing two structures, the LGA algorithm generates many different local superpositions to detect regions where proteins are similar, and calculated similarity scores are not affected by some perturbations in small parts of compared proteins. In essence, LGA assesses structure similarity based on detected conserved parts between two proteins or protein fragments while removing small deviating regions from calculated scores. This capability of LGA allows accurate detection of similar pocket shapes. The main metrics to assess confidence in detected pockets are a scoring function LGA_S [a combination of global distance test and longest continuous segment measures (28)], which evaluates structure similarities on C-alpha and/or C-beta levels, and GDC [global distance calculations (29)], which allows evaluation on an all-atom level, i.e. extending structure similarity evaluation to the conformation of side chain atoms.

When applied to predict protein binding sites in a given protein structure, PDBspheres detects ligand–protein binding regions using the pocket/sphere templates from the PDBspheres library constructed from all available structures deposited in the PDB database. After a binding pocket is detected, the ligand(s) from matching template(s) is/are inserted into the identified pocket in a query protein to illustrate an approximate location of the ligand. The location is approximate because it is based on the alignment of the query protein with the template protein spheres, and no docking or any energy minimization or structure relaxation is undertaken. Thus, it should be noted that PDBspheres is not a docking system to predict *de novo* ligand poses within a binding site. However, further relaxation of the predicted protein–ligand complex can be considered as the next step to improve a ligand placement within a pocket (which is a subject of continuing PDBspheres system development).

In the process of detecting pocket candidates within protein structures, similarity searches can be performed using all templates in the PDBspheres library (i.e. exhaustive search, testing all 2.0 M pockets from the library), or if time is prohibitive, searches can be performed on a preselected subset of the sphere templates. For example, the preselec-

Table 1. Median of family median *F* scores and MCCs for apo and holo datasets for all seven ‘non-template-based’ LBS prediction methods described in (25) and PDBspheres (for which mean values are also given, the second line in the rows for PDBspheres)

Method	Apo		Holo		Apo		Holo	
	F	*F* IQR	*F*	*F* IQR	MCC	MCC IQR	MCC	MCC IQR
SURFNET	0.23	0.23	0.23	0.24	0.22	0.26	0.23	0.28
Ghecom	0.48	0.5	0.54	0.55	0.5	0.54	0.53	0.62
LIGSITE	0.48	0.46	0.52	0.48	0.46	0.52	0.5	0.56
Fpocket	0.42	0.57	0.53	0.56	0.43	0.61	0.51	0.62
Depth	0.4	0.29	0.42	0.27	0.38	0.29	0.4	0.27
AutoSite	0.35	0.59	0.45	0.6	0.34	0.67	0.42	0.67
Kalasanty	0.49	0.51	0.51	0.43	0.48	0.56	0.54	0.48
PDBspheres(100)	0.81	0.14	0.82	0.15	0.80	0.15	0.82	0.15
	0.80		0.82		0.79		0.81	
PDBspheres(90)	0.77	0.18	0.79	0.16	0.76	0.18	0.77	0.17
	0.73		0.74		0.72		0.73	
PDBspheres(80)	0.76	0.17	0.78	0.18	0.75	0.18	0.77	0.18
	0.72		0.73		0.71		0.72	
PDBspheres(70)	0.76	0.19	0.78	0.17	0.75	0.19	0.77	0.17
	0.71		0.73		0.70		0.72	
PDBspheres(60)	0.76	0.19	0.78	0.17	0.75	0.19	0.77	0.17
	0.71		0.72		0.70		0.72	
PDBspheres(50)	0.75	0.20	0.77	0.17	0.74	0.20	0.75	0.19
	0.70		0.71		0.69		0.70	

Interquartile range (IQR) describes the difference between maximum and minimum scores within the middle 50% of values when ordered from lowest to highest. IQR indicates how close the middle 50% of family *F* and MCC values are to their respective medians. *F* and MCC scores are described in the ‘Benchmark dataset and evaluation metrics’ section.

tion process can be based on specific targeted ligands (e.g. their names or sizes) or can be limited to those template spheres from the PDBspheres library that come from homologous proteins. The computational time of the structure processing can vary depending on the size of the protein or the number of template spheres from the PDBspheres library preselected by the system for the pocket detection and similarity evaluation. An exhaustive search (against the entire PDBspheres library) can take >1 day on a single processor machine; however, with the above-mentioned preselection procedures, the calculations can be completed in <1 h for medium size proteins. For example, the processing of three protein structures discussed in the manuscript and illustrated in Figure 1 (neuropilin-1, 158aa), Figure 2 (PL2pro, 318aa) and Figure 6 (tryptase, 248aa) took 7, 52 and 50 min, respectively, on a single processor with a 16-core machine.

The clustering of identified pocket–sphere matches and their corresponding ligands characterizes distinct pocket regions within the protein by the sets of residues interacting with inserted ligands. The clustering of interacting residues allows identification of overlapping parts of ligands that approximate the ligand’s ‘core’ conformation within detected pockets and for each cluster defines a representative set of residues forming a consensus pocket. An example of an identified cluster of pocket spheres is shown in Figure 2. Each protein may have more than one such consensus pocket.

PDBspheres library

Each protein–ligand template sphere in the PDBspheres library is a subset of the records from a corresponding PDB entry, consisting of the coordinates of all atoms belonging to a given ligand and coordinates of all protein atoms belonging to residues near that ligand (water atoms are excluded). The protein residue is part of the sphere if at least one of its atoms is within 12.0 Å of any atom of the ligand. Previous research indicated that distances of 7.5 Å are sufficient to capture informative functional properties for clustering purposes (30); however, based on our experimentation using the LGA program for detecting local structure similarities, we expanded the distance to 12.0 Å. This size of the ‘template sphere’ is sufficient to capture local structural environment of the ligand for protein structure comparative needs. Our tests indicated that >12 Å spheres would affect accuracy in calculated structure conformation-based local residue–residue correspondences between template spheres and the query protein within detected pockets’ regions. On the other hand, the <12 Å distance criteria may not provide sufficient fold constraints to capture the uniqueness of searched pockets. To assist in identification of functional residues, PDBspheres also collects and reports information on protein–ligand interface residues. These residues are identified as those of which at least one atom is within 4.5 Å of any ligand atom.

In the PDBspheres library, the 12.0 Å ‘sphere’ entries have been constructed for each ligand in the PDB, including peptides, metals and ions, although the library includes only peptides containing 25 or fewer residues. The library is updated weekly in coordination with new PDB releases. As of 13 October 2021, the library consisted of 2 069 796 spheres (binding site templates).

The primary use of the PDBspheres library is to identify ‘sphere’ protein structures that are structurally similar to regions of a query protein structure. The query protein structure may be a complete, multimeric assembly, or it may be a single subunit of such an assembly, or even a fragment of a protein as long as it carries enough structural information (local structure conformation formed by atom coordinates) to reflect a structural shape of a putative binding site.

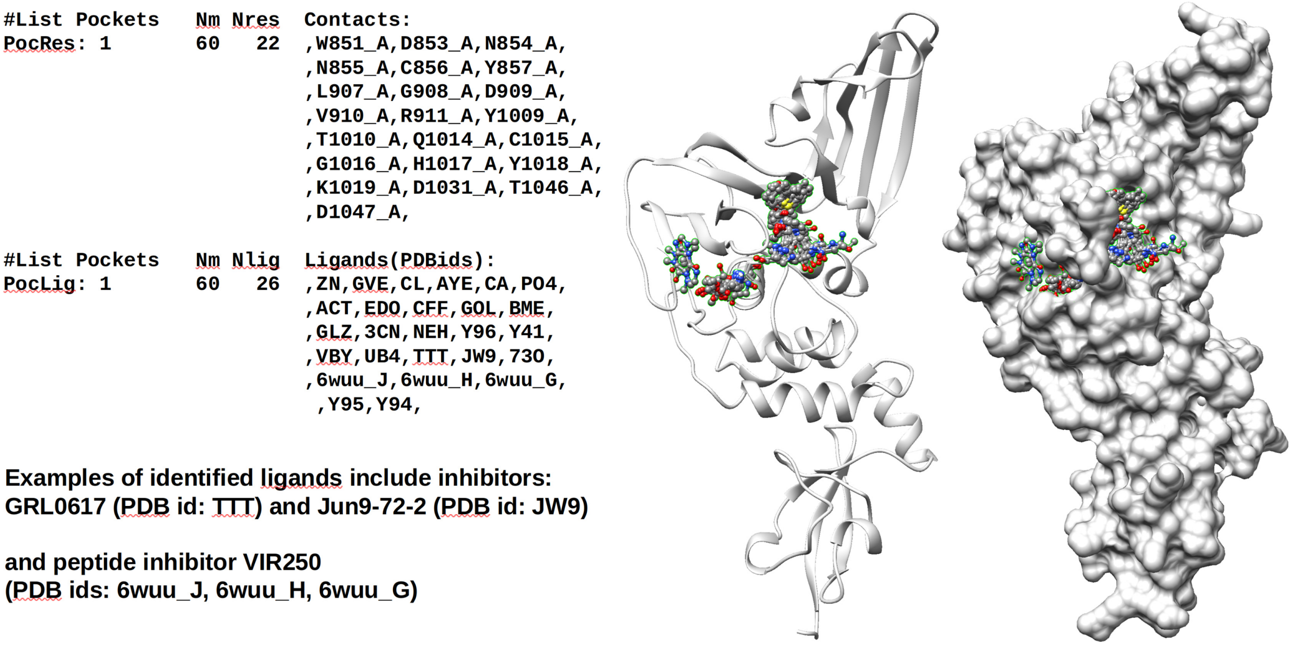

```
#List Pockets   Nm Nres  Contacts:
PocRes: 1       60   22  ,W851_A,D853_A,N854_A,
                         ,N855_A,C856_A,Y857_A,
                         ,L907_A,G908_A,D909_A,
                         ,V910_A,R911_A,Y1009_A,
                         ,T1010_A,Q1014_A,C1015_A,
                         ,G1016_A,H1017_A,Y1018_A,
                         ,K1019_A,D1031_A,T1046_A,
                         ,D1047_A,

#List Pockets   Nm Nlig  Ligands(PDBids):
PocLig: 1       60   26  ,ZN,GVE,CL,AYE,CA,PO4,
                         ,ACT,EDO,CFF,GOL,BME,
                         ,GLZ,3CN,NEH,Y96,Y41,
                         ,VBY,UB4,TTT,JW9,73O,
                         ,6wuu_J,6wuu_H,6wuu_G,
                          ,Y95,Y94,
```

Examples of identified ligands include inhibitors: GRL0617 (PDB id: TTT) and Jun9-72-2 (PDB id: JW9)

and peptide inhibitor VIR250 (PDB ids: 6wuu_J, 6wuu_H, 6wuu_G)

Figure 2. Identified in PL2pro pocket cluster #1. A list of identified ligands includes three important inhibitors: GRL0617, Jun9-72-2 and VIR250. Agreement in sets of contact residues is also observed (see Figure 4).

PDBspheres similarity searches

The fundamental identification method used by PDBspheres is structural alignment of a sphere with the query protein structure and the assessment of the structural match. For a general use, a comprehensive search—i.e. a structural alignment-based search of the entire PDBspheres library (over 2 million sphere templates)—would be computationally expensive. One means to address this issue is to conduct an initial search for matches to a query protein structure on a subset of sphere templates. Then, if needed, the search can be expanded to additional templates from the library. In its current implementation for possibly faster processing, the PDBspheres library searches can be restricted to a subset of template spheres selected based on (i) ligand specificity, e.g. ligand names, their sizes or similarities, or (ii) sequence similarity between the query protein and PDB proteins from which the PDBspheres library entries were derived. In the latter approach, the sequence similarity searches are conducted using the Smith–Waterman algorithm against FASTA-format sequences of all proteins contributing to the PDBspheres library entries. In the current version of PDBspheres, the Smith–Waterman algorithm ‘ssearch36’ (31) is used.

In the PDBspheres library, each sphere template entry includes a number of characteristics such as the ligand name (PDB ligand ID), the number of heavy atoms in the ligand and the number of residues in the protein fragment forming the protein–ligand ‘sphere’ (i.e. the size of the pocket template). Thus, the list of matching spheres can be screened using specific criteria related to the expected pocket size, exact ligand name or ligand similarity. A selection of the template spheres based on the estimated similarity between the expected ligand and the PDB ligands from the PDBspheres system can be quantified by the Tanimoto or Tversky similarity indexes (32).

After a selection of template spheres is completed, each member of this set is evaluated by assessing its structure similarity with a query protein. The evaluation is performed in two steps: (i) detection of the region resembling the binding site shape and (ii) assessment of the similarity in residue conformations including a conformation in their side chain atoms. The primary search involves a calculation of structural alignment between template spheres and a query protein. The structural alignment is conducted using the LGA program and is calculated using a single point representation of aligning residues (C-alpha atoms, C-beta atoms or any other point that can represent a residue position). The structural similarity search returns similarity scores (LGA_S) and alignments between template spheres of various pockets and the query protein. The final evaluation of identified pockets is done by assessing similarities in the conformation of all atoms (including side chain atoms) using the GDC metric.

The PDB ligand from the sphere template is translated and rotated according to the transformation that results from aligning the sphere template atoms to the query protein atoms. The ligand atoms are not considered in this alignment, and their conformation is not altered. It means that potential steric clashes between protein residues and atoms of ‘inserted’ ligands can be observed. The number of possible clashes is reported.

PDBspheres reports the following set of characteristics for all pockets detected within a given protein:

1. PDB identifier of the protein structure from which a template sphere matching the query protein pocket was derived.

2. PDB identifier of the ligand from the template sphere matching the query protein pocket.
3. List of residues in the query protein in direct contact with the inserted ligand (residues within the distance ≤4.5 Å).
4. Coordinates of the centroid of the ligand inserted into the detected pocket in the query protein.

Because the pocket searches can match template spheres to different regions of the query protein, all identified pocket candidates are organized into clusters. Within the PDBspheres approach, the merging and clustering of individually detected pockets (i.e. pockets detected based on individual template spheres) is performed to satisfy the following two criteria:

1. Within each cluster, the pockets are grouped together based on sets of query protein residues interacting with inserted ligands. When >80% of predicted contact residues are the same, then these sets are merged to define residues forming the pocket.
2. Pockets and the sets of residues identified as in contact with ligands are merged when the inserted ligands overlap (the distances between ligand centroids are not larger than 2.0 Å).

This grouping of pockets and their corresponding inserted ligands allows to define sets of residues interacting with similar ligands and also helps identify overlapping parts of different ligands. Such overlapping parts can approximate the ligand's 'core' conformation, whose protein contact residues can be used to define representative (consensus) pockets within the protein.

For a given protein, the following set of measurements and scorings are provided to help assess the confidence level of the pocket prediction (see examples provided in Figure 4 and Supplementary File S1):

- LIGAND: protein–ligand template sphere identifier that includes PDB ID of the ligand, ligand size and PDB ID of the protein–ligand complex from which the sphere was extracted.
- Ns: number of residues forming the protein–ligand template sphere.
- RMSD: root mean square deviation calculated on superimposed C-alpha or C-beta atoms from sphere template and detected protein pocket.
- Nc: number of conserved, i.e. 'tightly' superimposed, residue pairs between the template sphere and detected pocket in an evaluated protein.
- SeqID: sequence identity in structure aligned conserved residues. The higher value indicates that the protein forming a template sphere and the query protein might be close homologues.
- LGA: structure similarity score based on aligned by the LGA program C-alpha or C-beta atoms.
- GDC: structure similarity score calculated by the LGA program assessing agreement in conformations of all atoms (i.e. including side chain atoms).
- N4: the number of predicted protein–ligand contact residues (i.e. query protein residues observed within 4.5 Å of the inserted ligand).
- cl: the number of query protein residues that may have possible steric clashes with inserted ligand's atoms.

First, to be considered a predicted site candidate, there must be at least 10 aligned residues ($Nc \geq 10$) that are conserved between the query protein and the sphere. Second, the structural similarity measured by GDC (29), which counts how many atoms (including side chain atoms) in the query protein and the template sphere are in close superposition, must be at least 55% ($GDC \geq 55.0$). Third, there must be at least one query protein binding site residue that has an atom within <4.5 Å of the atom of the inserted PDB ligand ($N4 \geq 1$). Finally, there are no more than two steric clashes ($cl \leq 2$) (distance <1.0 Å) allowed between query protein binding site residue atoms and any atom of the inserted ligand. The 'cl' number is counted per residue, which means that multiple clashing atoms, all within a single residue, are allowed, but not more than two residues can be involved in clashes.

We may expect a higher confidence in predicted binding sites when $Nc \geq 25$, $GDC \geq 65$ and $cl \leq 1$. Note that these thresholds cannot be considered as absolute requirements. For example, possible clashes indicated by '$cl > 0$' may suggest a need to correct the placement of the inserted ligand. Ideally, a score of '$cl = 0$' would enhance the confidence in ligand–protein binding prediction; however, in many cases when '$cl > 0$' the ligand placement within the pocket can be fixed by additional adjustment or refinement of protein side chain atoms through docking or molecular dynamics simulations. It is also important to keep in mind that the query protein structure may not be in its 'holo' conformation to properly accommodate the ligand (i.e. without clashes), so the conformation of binding site residues of the protein may require more substantial optimization. Indeed, recent studies of ligand binding site refinements show significant success in generating reliable 'holo' (ligand-bound) protein structures from their 'apo' (ligand-free) conformations (33).

If N4—the number of protein atoms within 4.5 Å of the ligand—is very low, then this indicates that the current placement of the ligand does not show strong interactions with residues of the protein binding site. This may suggest that the pocket is too large (or some residues in the protein model are missing, or side chain atoms are not in the right conformation). Of course, it may also indicate that the identified pocket is incorrect, or the location of the inserted ligand is wrong, but these conclusions can only be confirmed by more detailed inspection. In such cases, it can be informative to check the overlap of the template sphere pocket and the query protein pocket (i.e. check the Nc number of conserved superimposed pocket-forming residues). Higher overlaps (e.g. $Nc \geq 25$) indicate greater size of the region forming the pocket and thus the higher confidence in reported pocket similarities (more residues identified as conserved). However, such thresholds cannot be decided upfront because in cases of shallow cavities or interface sites on the surface of the protein, the Nc number can be low.

The application of the PDBspheres for binding site detection in papain-like proteinase (PL2pro) from COVID-19 is illustrated in Figures 2–4. In Figure 2, we show results from detected pocket cluster #1, which was defined based on PL2pro pocket structure similarities with 60 pocket–ligand template spheres ($Nm = 60$). The number of predicted dif-

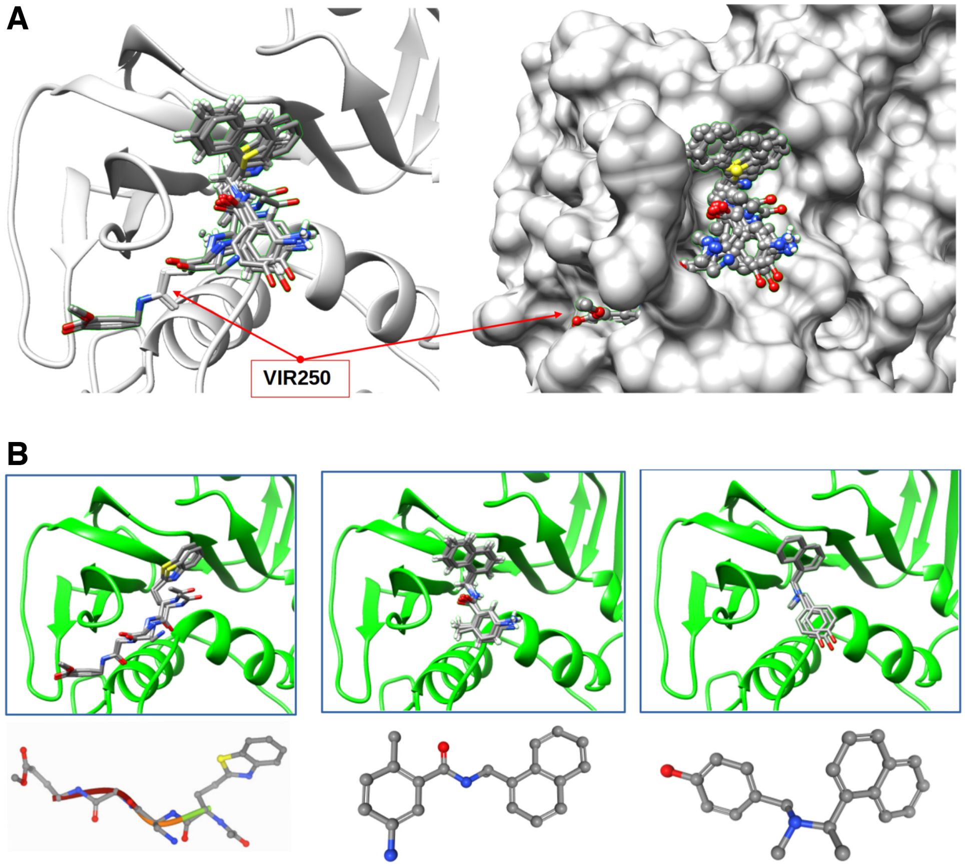

Peptide inhibitor VIR250
PDB ids: 6wuu_J, 6wuu_H, 6wuu_G

Inhibitor GRL0617
PDB id: TTT

Inhibitor Jun9-72-2
PDB id: JW9

Figure 3. (**A**) Example of the peptide inhibitor VIR250 that passes through the 'gorge'. Inhibitors GRL0617 and Jun9-72-2 are placed only on one side (right part) of the cavity of pocket cluster #1. (**B**) Assessed by PDBspheres, poses of all three ligands that come from different template spheres show strong overlap.

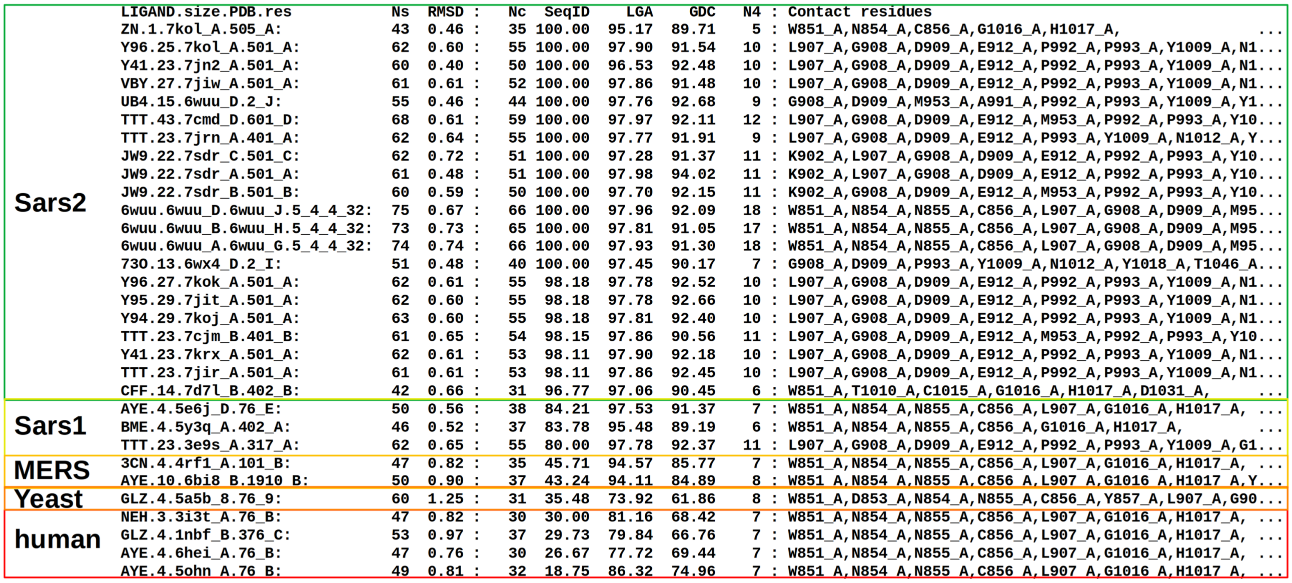

```
        LIGAND.size.PDB.res            Ns  RMSD :   Nc  SeqID    LGA    GDC   N4 : Contact residues
        ZN.1.7kol_A.505_A:             43  0.46 :   35 100.00  95.17  89.71    5 : W851_A,N854_A,C856_A,G1016_A,H1017_A,            ...
        Y96.25.7kol_A.501_A:           62  0.60 :   55 100.00  97.90  91.54   10 : L907_A,G908_A,D909_A,E912_A,P992_A,P993_A,Y1009_A,N1...
        Y41.23.7jn2_A.501_A:           60  0.40 :   50 100.00  96.53  92.48   10 : L907_A,G908_A,D909_A,E912_A,P992_A,P993_A,Y1009_A,N1...
        VBY.27.7jiw_A.501_A:           61  0.61 :   52 100.00  97.86  91.48   10 : L907_A,G908_A,D909_A,E912_A,P992_A,P993_A,Y1009_A,N1...
        UB4.15.6wuu_D.2_J:             55  0.46 :   44 100.00  97.76  92.68    9 : G908_A,D909_A,M953_A,A991_A,P992_A,P993_A,Y1009_A,Y1...
        TTT.43.7cmd_D.601_D:           68  0.61 :   59 100.00  97.97  92.11   12 : L907_A,G908_A,D909_A,E912_A,M953_A,P992_A,P993_A,Y10...
        TTT.23.7jrn_A.401_A:           62  0.64 :   55 100.00  97.77  91.91    9 : L907_A,G908_A,D909_A,E912_A,P993_A,Y1009_A,N1012_A,Y...
        JW9.22.7sdr_C.501_C:           62  0.72 :   51 100.00  97.28  91.37   11 : K902_A,L907_A,G908_A,D909_A,E912_A,P992_A,P993_A,Y10...
        JW9.22.7sdr_A.501_A:           61  0.48 :   51 100.00  97.98  94.02   11 : K902_A,L907_A,G908_A,D909_A,E912_A,P992_A,P993_A,Y10...
        JW9.22.7sdr_B.501_B:           60  0.59 :   50 100.00  97.70  92.15   11 : K902_A,G908_A,D909_A,E912_A,M953_A,P992_A,P993_A,Y10...
Sars2   6wuu.6wuu_D.6wuu_J.5_4_4_32:   75  0.67 :   66 100.00  97.96  92.09   18 : W851_A,N854_A,N855_A,C856_A,L907_A,G908_A,D909_A,M95...
        6wuu.6wuu_B.6wuu_H.5_4_4_32:   73  0.73 :   65 100.00  97.81  91.05   17 : W851_A,N854_A,N855_A,C856_A,L907_A,G908_A,D909_A,M95...
        6wuu.6wuu_A.6wuu_G.5_4_4_32:   74  0.74 :   66 100.00  97.93  91.30   18 : W851_A,N854_A,N855_A,C856_A,L907_A,G908_A,D909_A,M95...
        73O.13.6wx4_D.2_I:             51  0.48 :   40 100.00  97.45  90.17    7 : G908_A,D909_A,P993_A,Y1009_A,N1012_A,Y1018_A,T1046_A...
        Y96.27.7kok_A.501_A:           62  0.61 :   55  98.18  97.78  92.52   10 : L907_A,G908_A,D909_A,E912_A,P992_A,P993_A,Y1009_A,N1...
        Y95.29.7jit_A.501_A:           62  0.60 :   55  98.18  97.78  92.66   10 : L907_A,G908_A,D909_A,E912_A,P992_A,P993_A,Y1009_A,N1...
        Y94.29.7koj_A.501_A:           63  0.60 :   55  98.18  97.81  92.40   10 : L907_A,G908_A,D909_A,E912_A,P992_A,P993_A,Y1009_A,N1...
        TTT.23.7cjm_B.401_B:           61  0.65 :   54  98.15  97.86  90.56   11 : L907_A,G908_A,D909_A,E912_A,M953_A,P992_A,P993_A,Y10...
        Y41.23.7krx_A.501_A:           62  0.61 :   53  98.11  97.90  92.18   10 : L907_A,G908_A,D909_A,E912_A,P992_A,P993_A,Y1009_A,N1...
        TTT.23.7jir_A.501_A:           61  0.61 :   53  98.11  97.86  92.45   10 : L907_A,G908_A,D909_A,E912_A,P992_A,P993_A,Y1009_A,N1...
        CFF.14.7d7l_B.402_B:           42  0.66 :   31  96.77  97.06  90.45    6 : W851_A,T1010_A,C1015_A,G1016_A,H1017_A,D1031_A,     ...
        AYE.4.5e6j_D.76_E:             50  0.56 :   38  84.21  97.53  91.37    7 : W851_A,N854_A,N855_A,C856_A,L907_A,G1016_A,H1017_A, ...
Sars1   BME.4.5y3q_A.402_A:            46  0.52 :   37  83.78  95.48  89.19    6 : W851_A,N854_A,N855_A,C856_A,G1016_A,H1017_A,        ...
        TTT.23.3e9s_A.317_A:           62  0.65 :   55  80.00  97.78  92.37   11 : L907_A,G908_A,D909_A,E912_A,P992_A,P993_A,Y1009_A,G1...
MERS    3CN.4.4rf1_A.101_B:            47  0.82 :   35  45.71  94.57  85.77    7 : W851_A,N854_A,N855_A,C856_A,L907_A,G1016_A,H1017_A, ...
        AYE.10.6bi8_B.1910_B:          50  0.90 :   37  43.24  94.11  84.89    8 : W851_A,N854_A,N855_A,C856_A,L907_A,G1016_A,H1017_A,Y...
Yeast   GLZ.4.5a5b_8.76_9:             60  1.25 :   31  35.48  73.92  61.86    8 : W851_A,D853_A,N854_A,N855_A,C856_A,Y857_A,L907_A,G90...
        NEH.3.3i3t_A.76_B:             47  0.82 :   30  30.00  81.16  68.42    7 : W851_A,N854_A,N855_A,C856_A,L907_A,G1016_A,H1017_A, ...
human   GLZ.4.1nbf_B.376_C:            53  0.97 :   37  29.73  79.84  66.76    7 : W851_A,N854_A,N855_A,C856_A,L907_A,G1016_A,H1017_A, ...
        AYE.4.6hei_A.76_B:             47  0.76 :   30  26.67  77.72  69.44    7 : W851_A,N854_A,N855_A,C856_A,L907_A,G1016_A,H1017_A, ...
        AYE.4.5ohn_A.76_B:             49  0.81 :   32  18.75  86.32  74.96    7 : W851_A,N854_A,N855_A,C856_A,L907_A,G1016_A,H1017_A, ...
```

Figure 4. Fragment of the PDBspheres summary table reporting predicted PL2pro ligands assigned to pocket cluster #1. Results highlighted in green (when SeqID > 95) indicate that similar pockets are detected in Sars2 or variants of Sars2. When SeqID < 30 (results highlighted in red), examples of similar pockets detected in human proteins are shown. An agreement in sets of contact residues indicates that all listed ligands are predicted to bind the same pocket identified through clustering as 'pocket cluster #1'.

ferent bound ligands is Nlig = 26, and the combined total number of residues being in contact with bound ligands is Nres = 22.

In Figure 3, we show that the poses of three inhibitors from pocket cluster #1 (VIR250, GRL0617, and Jun9-72-2, whose PDB IDs are 6wuu_J, TTT and JW9, respectively) overlap significantly. These ligand poses are brought from 11 different template spheres listed in Figure 4: 3 for VIR250, 5 for GRL0617 and 3 for Jun9-72-2.

In Figure 4, we present a snapshot (only 31 template spheres out of Nm = 60) from the summary table automatically created by the PDBspheres system for pocket cluster #1. A complete summary table of predicted pocket–ligands for a structural model of papain-like proteinase (PL2pro model: nCoV_nsp3.6w9c_A.pdb) is provided in Supplementary File S1.

Benchmark dataset and evaluation metrics

The benchmark dataset used to assess the performance of PDBspheres is the 'LBSp dataset' described in (25,26). It comprises 304 unique protein families (2528 structures in 1456 'holo' and 1082 'apo' conformations) with each family represented by several protein structures in different possible conformations. Since this LBSp dataset is curated, well designed, large and diverse, we have found it very suitable to test the performance of the PDBspheres method comprehensively.

The main criterion often used for the assessment of the accuracy of predictions of the binding site is the agreement in the set of residues predicted to be in contact with experimentally confirmed ligands [residue contacts derived from protein–ligand co-crystals from the PDB (27)]. To estimate the accuracy of our method, we followed the same metrics and evaluation procedures as used in (25). The authors defined reference lists called unified binding sites (UBS) as unions of all residues contacted by any bound ligands within the protein family. The scoring of binding site predictions is determined by agreement with the UBS reference using calculated numbers of residues: all residues predicted to be part of the binding site and confirmed in the experimental data are denoted as true positives (TP), all remaining residues (which are not predicted as part of the binding site and not confirmed in experimental data) are denoted as true negatives (TN), any residue predicted to be part of the binding site and not confirmed in experimental data is denoted as false positive (FP) or overprediction, and any remaining residues in the experimental data not accounted for in an algorithm's predicted binding site are denoted as false negatives (FN) or underpredictions.

Both MCCs and F scores as calculated by Equations (1) and (2) have been used as metrics to represent the predictive power of evaluated binding site prediction methods.

$$\mathrm{MCC} = \frac{(\mathrm{TP} \times \mathrm{TN}) - (\mathrm{FP} \times \mathrm{FN})}{\sqrt{(\mathrm{TP}+\mathrm{FP})(\mathrm{TP}+\mathrm{FN})(\mathrm{TN}+\mathrm{FP})(\mathrm{TN}+\mathrm{FN})}}, \quad (1)$$

$$F = \frac{2 \times \mathrm{TP}}{2 \times \mathrm{TP} + \mathrm{FP} + \mathrm{FN}}. \quad (2)$$

Of course, there are other metrics sometimes used to evaluate protein–ligand binding site detection successes, e.g. distance center–center (DCC) (34) and discretized volume overlap (DVO) (12). DCC is a metric to evaluate the correct location of the pocket based on the distance between the predicted and the actual center of the pocket (centroids). If DCC is below 4 Å, the pocket is considered as correctly located. DVO, on the other hand, is defined as the ratio of the volume of the intersection of the predicted and the actual segmentations to the volume of their union. It assesses the correctness of the shape of predicted pockets. However, in our study we follow metrics described in (25) as they focus on assessing accuracy of binding site prediction methods based on the correctness of identified pocket residues being in contact with ligands. Similar approaches were used in CASP experiments to evaluate the performance of binding site prediction methods.

RESULTS AND DISCUSSION

Performance of PDBspheres on LBSp dataset

In (25), predictive power of different methods is assessed using two metrics: F scores and MCCs. The F scores and MCCs provide a good description of the relative success of evaluated algorithms by assessing whether or not a method produced a predicted binding site that contains residues in common with the reference UBS list of ligand contact residues. They assign high scores not just when at least one residue in a given site is identified correctly, but rather reward methods with more correct and less false predictions of contact residues implying which of the algorithm pocket predictions are close to the 'correct' location on the binding surface of the protein. Note that a similar evaluation procedure using MCC scores between predicted and observed contact residues was also applied in CASP experiments.

Clark *et al.* (25) compared the following methods on their LBSp dataset: SURFNET (19), Ghecom (35), LIGSITE (36), Fpocket (37), Depth (38), AutoSite (39) and Kalasanty (15). Five of these methods are considered to be geometry based, while one is energy based, and one is machine learning based. To perform our analysis, we took prediction results for these seven methods from the supplementary data from (25). In Table 1, we present the prediction results for PDBspheres and recalculated—for consistency—F and MCC scores of the seven above-mentioned methods. The last six data rows in Table 1 show results from the evaluation of PDBspheres when the pocket detection was performed using the complete PDBspheres library (100%), and when the PDBspheres library was restricted to templates with no more than 90%, 80%, 70%, 60% and 50% sequence identity with query proteins, respectively. The six rows for PDBspheres include also the mean values of MCC in addition to the median values since this metric was used by CASP assessors.

Structural similarity of binding sites versus sequence identity

Here, we discuss how close in sequence identity two proteins need to be to have structurally similar binding sites, addressing these two questions:

- How low the level of sequence identity between two proteins can be and still share similar pockets and perform similar functions?

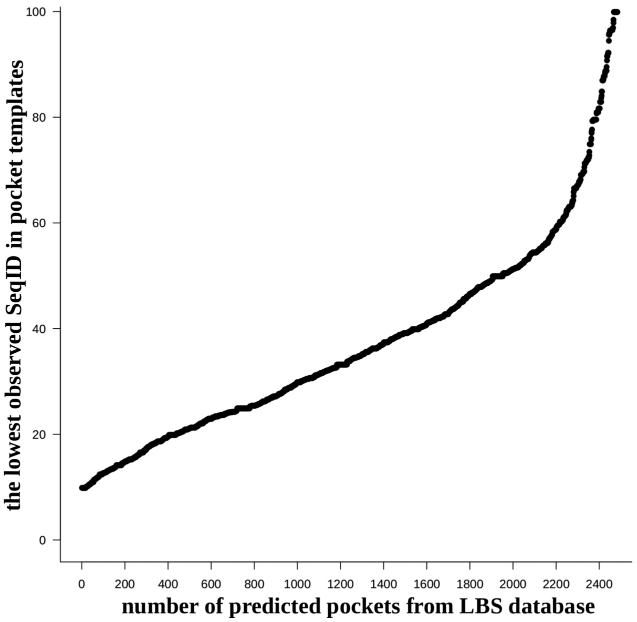

Figure 5. The plot illustrates how many pockets from the LBSp database proteins (all 2528 pockets; 'apo' and 'holo' combined) can be predicted based on binding site templates derived from proteins with lowest possible sequence identity to the query proteins. For example, at least 400 pockets (see left bottom part of the plot) can be predicted based on template binding sites derived from proteins that share as low as 20% SeqID with a query protein. On the other hand, >2400 pockets (∼95%) can be correctly predicted based on templates sharing no more than 80% of SeqID with query proteins in their binding site regions.

- Do such proteins have enough similarity in their functional sites to bind ligands in a similar manner?

Figure 5 illustrates results from the LBSp database pocket identification calculations, which were summarized in Table 1. These results illustrate that in contrast to the large diversity of possible protein sequences the number of structurally distinct pockets is limited; therefore, proteins that by sequence are very different may still share almost identical structural conformations in local regions (e.g. binding sites) and can perform similar functions. This observation served as a basis for the development of our PDBspheres structure template-based binding site detection method. The only limitation in its ability to identify correct pockets for a given protein might be an underrepresentation of particular pocket's conformation in currently experimentally solved protein structures deposited in the PDB database. For example, in case when a non-restricted library is used, the binding sites for all 304 families ('apo' and 'holo' protein conformations) were predicted. However, in the case of the restricted library (which excludes template spheres derived from proteins showing >90% sequence identity to the query proteins), the binding sites for five families of 'apo' versions and seven families of 'holo' versions were not predicted (see Table 2). In Table 2, we show even more results indicating that the protein binding sites are highly structurally conserved and can be successfully detected using structure-based template spheres taken from proteins sharing low sequence identity with targeted proteins. Even when the restrictions applied to the PDBspheres library increase from 90% to 50% sequence identity, the success in detecting the number of predicted pockets does not drop so rapidly. The same can be observed in Figure 5. More rapid decline in the ability to successfully detected pockets starts when the restriction on the library gets below 50% of sequence identity. Let us note that the main difference between results shown in Table 2 and Figure 5 is that the plot illustrates the correctness of the prediction (i.e. as accurate as possible identification of residues involved in protein–ligand interaction), while in Table 2 we report results from just detection of the pocket location in the protein (i.e. without any assessment of the accuracy and completeness of predicted interacting residues).

The PDBspheres method leverages this structure conservation quality efficiently. Indeed, thanks to the richness in diversity of protein structures deposited in the PDB, the system is able to identify location of 97% binding sites from the LBSp dataset using structural templates that share as low as 50% sequence identity with targeted proteins. Even with such significant restriction to the library of template spheres, the accuracy in identified sets of residues interacting with ligands is still high, ∼0.75 (median) and ∼0.7 (mean), as measured by *F* and MCC metrics (see Table 1).

As mentioned in (25), we expected that the template-based method such as PDBspheres could outperform non-template-based methods, which is evidenced in Table 1. We should emphasize, however, that PDBspheres is an exclusively structure-based method that does not utilize any prior information from libraries of sequences/residues forming binding sites. Additionally, PDBspheres does not use any prior information about the location of searched pockets in proteins from the same family. We treat all structures equally and independently (as pairwise comparisons) in finding structural similarities between the query protein and template spheres. Of course, we can find such cavities more easily in the 'holo' conformations, but as the results show, we can also find adequate structure similarities in 'apo' versions of the query protein, again strictly based on similarities in structure without any sequence-based knowledge of residues forming the pocket (residue information that could be transferred from some databases of 'holo' structures). All results reported here are based on PDBspheres superpositions calculated on C-alpha atoms. Results based on superposition of C-beta atoms (results not shown) are virtually identical.

In Figure 6, we show an example of correct pocket detection by PDBspheres using different pocket–ligand template spheres derived from proteins that share low sequence identity. Two compared proteins (serine proteases) have <38% of sequence identity, but they are structurally similar at the level of over 86% by LGA_S (assessment of similarity on the C-alpha atom level) and 77% by GDC (all-atom level). Of the residues that are in contact with corresponding ligands (distance below 4.5 Å) in the identified similar pockets, 11 out of 17 are identical (65%). The pocket template spheres come from two PDB complexes that bind inhibitor compounds having PDB ligand IDs 2A4 and QWE, respectively. These ligands are significantly different in size. Therefore, the distance between ligand centroids calculated from the complexes of the same orientations is very different; specifically, the distance between centroids of ligands when in-

Table 2. Number of detected pockets and pocket's families when the PDBspheres libraries are restricted to templates with sequence identity to proteins from the LBSp dataset not exceeding introduced cutoffs

Restricted sequence identity	Number of detected pockets			Number of pocket's families		
	All	Apo	Holo	All	Apo	Holo
100%	2528	1082	1456	304	304	304
90%	2481	1056	1435	299	299	297
80%	2469	1051	1428	298	296	297
70%	2469	1051	1428	298	296	297
60%	2464	1048	1426	297	295	296
50%	2457	1046	1421	295	294	294
	Percent of detected pockets			Percent of pocket's families		
50%	97.2%	96.7%	97.6%	97.0%	96.7%	96.7%

Results in this table reflect correctness in detection of just the pocket location in the protein, not an assessment of the accuracy and completeness of predicted interacting residues, which are reported in Table 1.

serted in any of these pockets is ~6.0 Å. However, the portions of the ligands inserted in pockets have a similar overlapping region and are in contact with similar amino acids from the pockets. In each of these two protein–ligand complexes, the core parts of the ligands are in contact with 13 residues, of which 11 are identical (85%) (see Figure 6C and E). We have had a similar observation in the example of human neuropilin-1 illustrated in Figure 1, when we focused on possible discrepancies in distances between centroids of two experimentally confirmed orientations of the same ligand inserted into the same pocket. The distance between 'core' parts of the ligand was very small, while the outside parts varied significantly. It suggests that if we are interested in identifying protein residues critical for ligand binding, we should concentrate mostly on those residues that are in contact with ligand's 'core' parts. Likewise, as shown in Figure 6, in case of different proteins and different ligands, a high sequence identity of residues being in contact with 'core' parts of the ligands can help identify those residues that may be critical for binding in similar pockets. These results illustrate how PDBspheres can be used to detect conservation in local structural conformations and to assess conservation of critical contact residues; both can assist in inferring protein function. These conclusions are also supported by results from evaluation of large and diverse set of proteins collected in the PDBbind dataset (40).

Clustering binding sites from PDBbind database

In this section, we describe how PDBspheres can be used to perform structure-based clustering and structure similarity analysis of binding sites from the PDBbind dataset (an extensive collection of experimentally measured binding affinity data for the protein–ligand complexes deposited in the PDB) (40) (ver. 2019). Some of these results were leveraged in our previous work generating rigorous training and validation datasets for machine learning of ligand–protein interactions (13). Here, we want to address the following questions:

- To what extent can structurally similar binding pockets having similar ligand placement allow inference of binding affinity from one pocket–ligand pair to another pocket–ligand pair?
- To what extent can clustering of detected pockets and calculated structure similarities among clustered pockets from different proteins provide functional information for protein annotation?

In our analysis, we focus on the 'refined' 2019 dataset (4852 structures), which we expanded by adding 24 structures from the previous PDBbind release that are not present in the 2019 version. Hence, in total the dataset of evaluated binding sites consists of 4876 structures. Since we are interested in the assessment of similarities between specific pockets listed in proteins from PDBbind (the PDBbind database reports only one pocket for each protein regardless of how many different pockets a given protein may have or how many alternative locations of a given pocket in a multichain protein complex can be observed), we restricted our structure similarity searches and evaluations to only those regions in PDBbind proteins that encompass targeted pockets. Note that many protein structures in the PDBbind refined dataset are multidomain complexes with total sizes of >2000 residues, so they can have multiple binding sites in addition to the targeted ones. Therefore, in our approach to evaluate similarities and cluster pockets from PDBbind, each of its protein structures was reduced to the region in the close vicinity of a reported ligand (residues having any atom within 16 Å of any ligand atom), and each ligand binding site reported in PDBbind was associated with its corresponding PDBspheres template sphere (residues having an atom within 12 Å of a ligand atom). We performed an all-against-all PDBspheres detection and pocket similarity evaluation using the 16 Å protein region representation of each PDBbind protein. Results from the pairwise pocket similarity evaluation are provided in Supplementary File S5. Structure similarity results allowed grouping of the 4876 PDBbind protein pockets into 760 clusters. Cluster details are provided in Supplementary Files S2–S4. Figure 7 illustrates the clusters, and it is a snapshot taken from the HTML Supplementary File S6 (interactive overview of predicted clusters created using 'plotly' R graphic library). Each axis of Figure 7 indexes a sample of 4876 protein pockets, where sampled protein names are reported to help identification of corresponding pockets or clusters in the plot. A 'zoom-in' option in the 'plotly' graph expands each rectangle to show a list of individual members of a selected cluster. It allows for each of the sampled proteins to be labeled with its exact location within the cluster, which is shown as the example in Figure 8. Further illus-

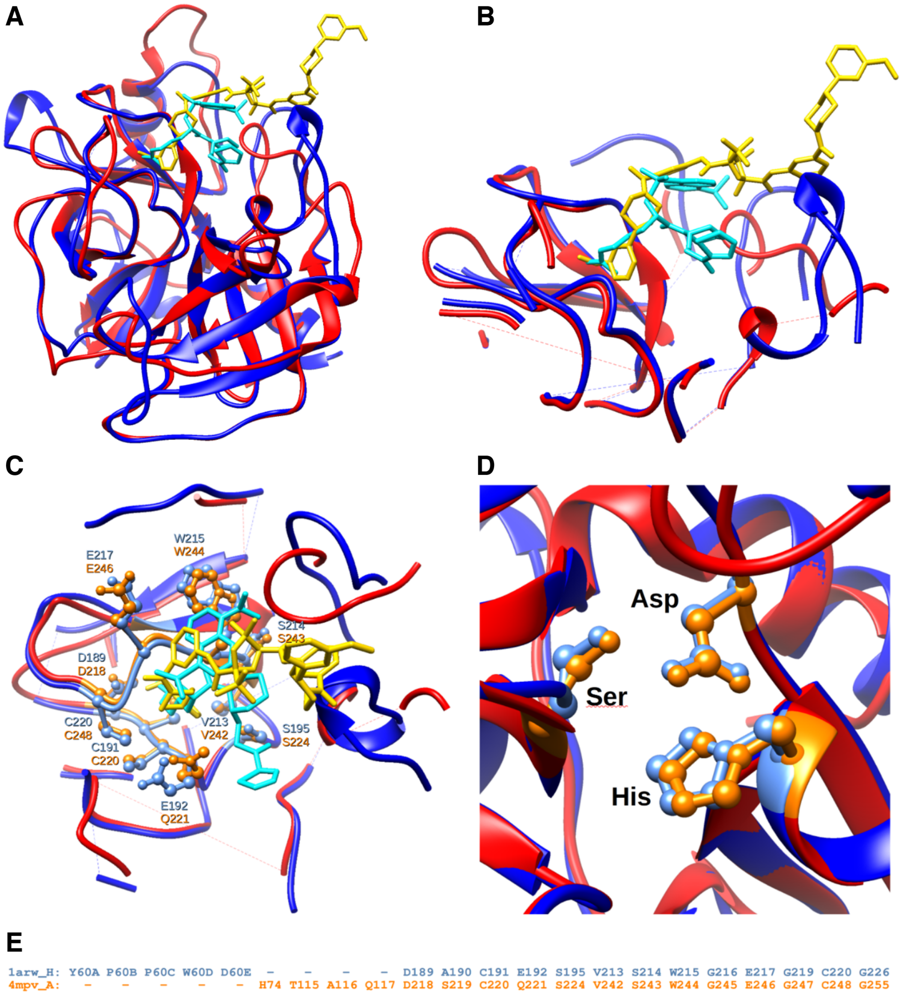

```
1arw_H: Y60A P60B P60C W60D D60E  -    -    -    -   D189 A190 C191 E192 S195 V213 S214 W215 G216 E217 G219 C220 G226
4mpv_A:   -    -    -    -    -  H74 T115 A116 Q117 D218 S219 C220 Q221 S224 V242 S243 W244 G245 E246 G247 C248 G255
```

Figure 6. Example of two structures of serine proteases: tryptase (in red PDB chain: 4mpv_A) and thrombin (in blue PDB chain: 1a4w_H) that share high structure similarity in their binding sites (over 77% by GDC), while the level of sequence identity between them is no higher than 38%. (**A**) Overall structure superposition of two protein–ligand complexes showing location of bound inhibitors. (**B**) PDBspheres-based local superposition of corresponding protein spheres surrounding ligands. (**C**) Structurally superimposed spheres of 4mpv and 1a4w show significant similarity in side chain conformation of residues interacting with corresponding ligands 2A4 and QWE. Residues interacting with ligands 2A4 and QWE are highlighted in orange and light blue, respectively. (**D**) Local superposition indicates a perfect agreement in the nearby catalytic triad residue conformations (His, Asp, Ser). (**E**) Structural alignment of residues from close distance (4.5 Å) from the corresponding ligands shows that 11 out of 13 (85%) residues that are in contact with similar core parts of the ligands are identical.

trations can be found in Supplementary File S6. Each rectangle in Figure 7 represents a cluster and is composed of small markers—one for each sampled protein–pocket pair within the cluster—colored by the GDC all-atom similarity score between each member of the cluster, where colors closer to red indicate a higher degree of similarity between members. For example, the first three large rectangles at the bottom left of Figure 7 represent predicted clusters: clusters #22 (318 members), #8 (351 members) and #5 (322 members), respectively. Evaluation of predicted clusters, which is reported in Supplementary File S2, shows that all members of cluster #22 are enzymes that belong to EC subclass 4.2.1.1, members of cluster #8 belong to EC subclass 3.4.21 and members of cluster #5 belong to EC subclass 3.4.23. All clusters along the diagonal in Figure 7 have high within-cluster similarity and are separated from other clusters according to the applied 'exclusive' clustering approach. Some of automatically created by PDBspheres clusters are formed by grouping together proteins from several 'finer' subclusters. For example, at the top right there is a large cluster (#25) with 382 members assigned to several subclasses of the broad-spectrum transferases—EC class 2.7 ('Transferring phosphorus-containing groups'), with varying degrees of similarity among its members as they belong to different and more specific subclasses that are still similar enough (according to the selected thresholds) to form one distinct cluster (#25). Data used in Figure 7 are reported in Supplementary Files S2 and S6.

As an example of results from PDBspheres clustering, Figure 8 shows a 'zoom-in' to cluster #277 (circled and marked by an arrow in Figure 7), which contains 24 protein–ligand pairs. This 'zoom-in' shows details of PDBbind binding sites grouped together based on all-against-all structure similarity measured by the

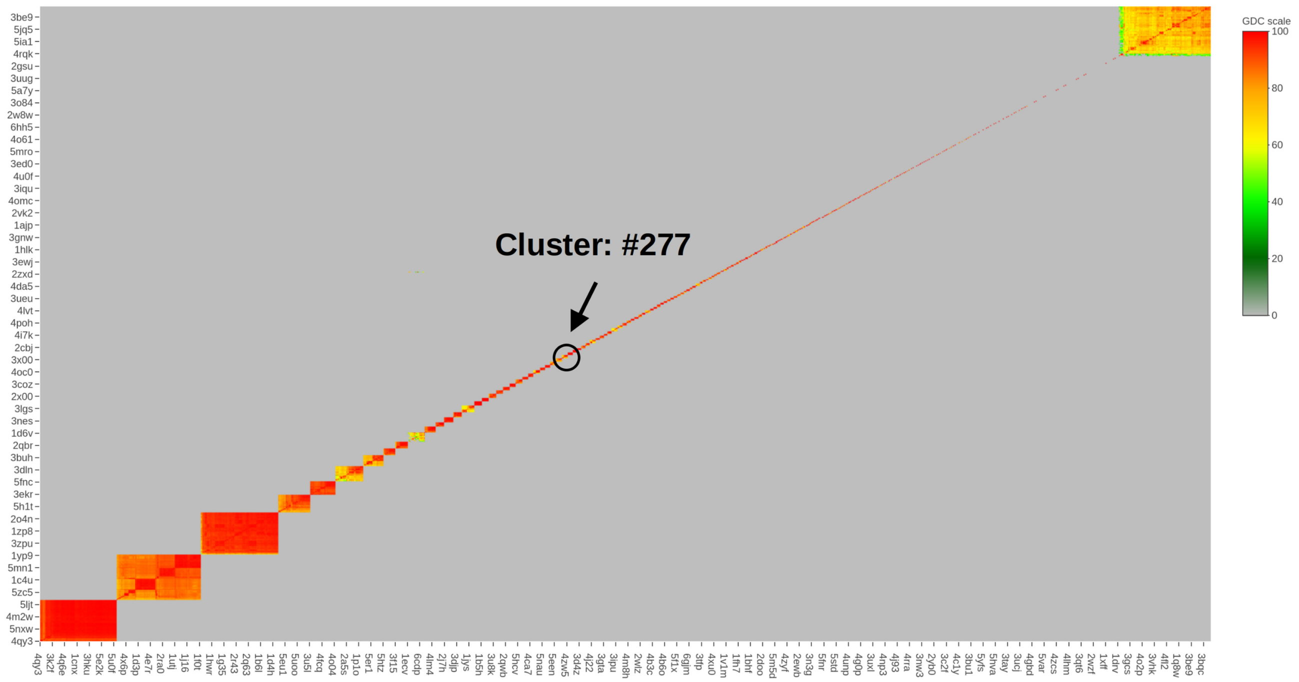

Figure 7. Clustering of the refined set of 4876 pockets from the PDBbind based on their structure similarity. PDBspheres-based pocket detection and similarity evaluation resulted in 760 constructed clusters. HTML file allowing interactive overview of predicted clusters is provided in Supplementary File S6. Figure 8 shows a 'zoom-in' to cluster #277, which contains 24 protein–ligand pairs.

4zw7	**:3.4.11.-:**
4zx4	**:3.4.11.-:**
4zw8	**:3.4.11.-:**
3ebi	**:3.4.11.-:**
4zw5	**:3.4.11.-:**
3ebh	**:3.4.11.-:3.4.11.2:**
4zw6	**:3.4.11.-:**
4r5t	**:3.4.11.-:**
2zxg	**:3.4.11.2:**
4k5p	**:3.4.11.-:**
4zx3	**:3.4.11.-:**
6eed	**:3.4.11.-:3.4.11.2:**
3t8v	**:3.4.11.-:**
3q44	**:3.4.11.-:**
4kxb	**:3.4.11.7:**
4kx8	**:3.4.11.1:3.4.11.2:**
4fys	**:3.4.14.-:3.4.11.2:**
4ou3	**:3.4.11.2:**
2vj8	**:3.3.2.6:3.4.11.4:**
2r59	**:3.3.2.6:3.4.11.4:**
3fh7	**:3.3.2.6:3.4.11.4:**
3b7r	**:3.3.2.6:3.4.11.4:**
3b7u	**:3.3.2.6:3.4.11.4:**
4l2l	**:3.3.2.6:3.4.11.4:**

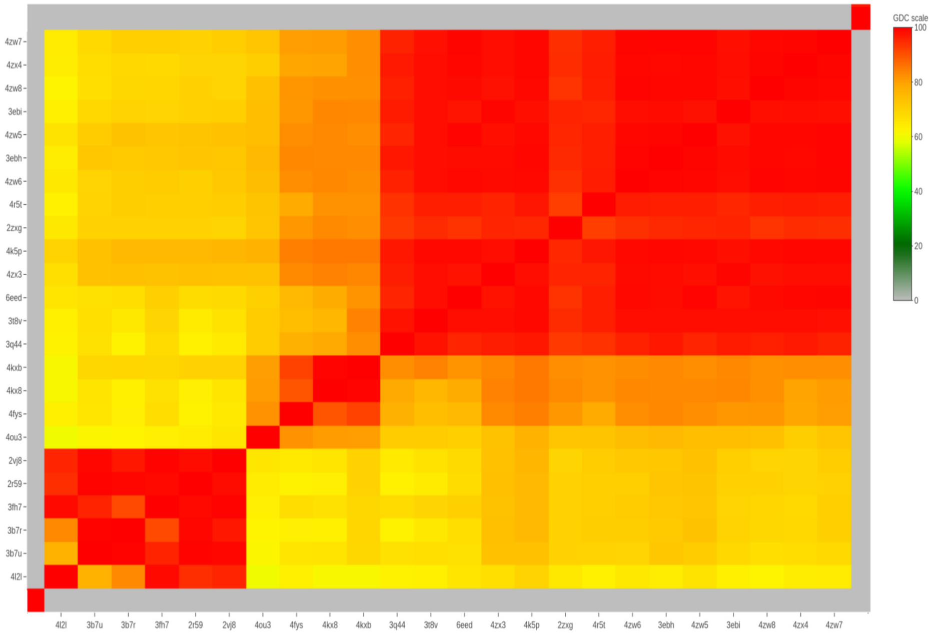

Figure 8. 'Zoom-in' to cluster #277 identified by PDBspheres in PDBbind dataset (see Figure 7 and Supplementary File S2). All 24 proteins within this cluster belong to the same enzyme subclass (3.4). The first column provides PDB IDs of each enzyme from the cluster. Corresponding EC numbers are reported in the second column, where alternative EC assignments are separated by colon. Coloring in the plot reflects pairwise similarity scores between clustered proteins as measured by GDC.

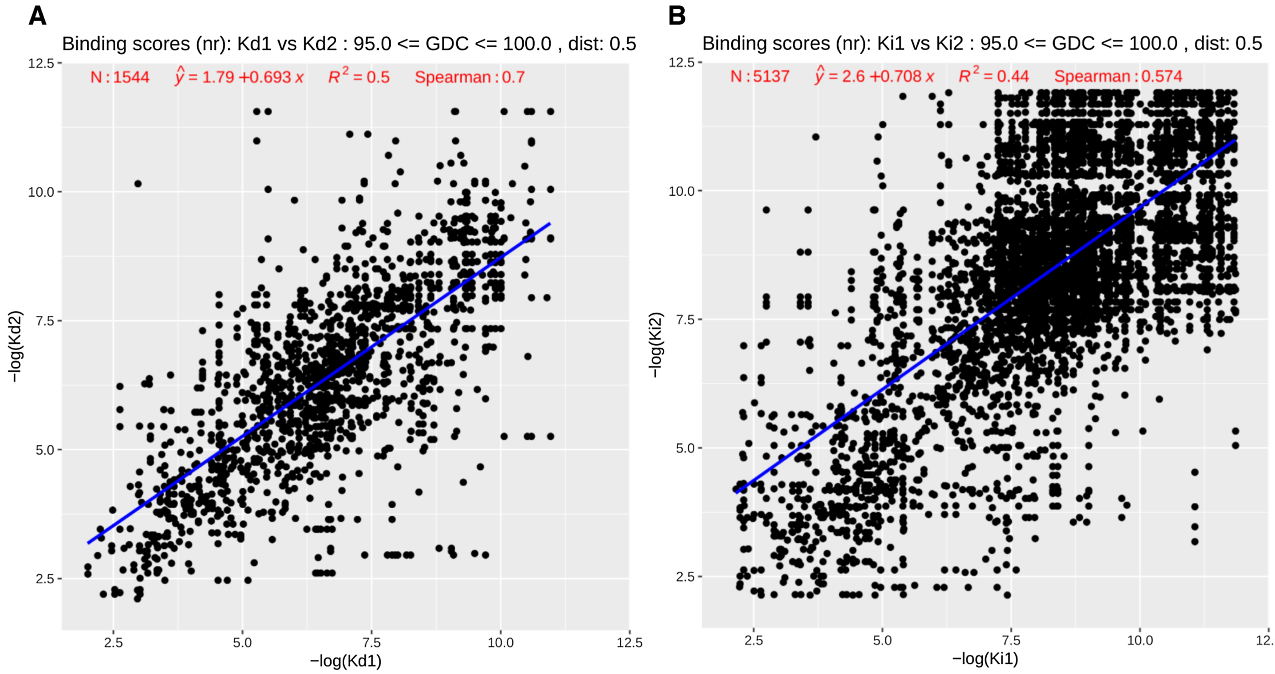

Figure 9. Scatter plots of (**A**) K_{d} values from 1544 pocket pairs and (**B**) K_{i} values from 5137 pocket pairs. Results shown in the plot were calculated for pairs satisfying the following similarity constraints: pocket GDC similarities ≥95% and ligand centroid's distance cutoff of 0.5 Å. Redundant pairs—self-comparisons and symmetry duplicates—are removed from calculations.

GDC score. Each of the proteins grouped into this cluster shares the same EC subclass (3.4) and GO annotation (:0006508:0008237:0008270:), which indicates that the PDBspheres-based clustering can assist in making predictions useful in protein functional annotation. The details of cluster #277 are reported in Supplementary Files S2 and S4. As shown in the plot, all 24 proteins belong to the same enzyme subclass (3.4)—hydrolases that act on peptide bonds; specifically, hydrolases with EC subclass 3.4.11 cleave off the N-terminal amino acid from a polypeptide. In addition to the general functional clustering of proteins, the PDBspheres clustering approach provides finer subclustering of proteins within predicted clusters. The bottom six proteins from cluster #277 form a clear subcluster as they share additional EC subclass 3.3.2.6—bifunctional zinc metalloprotease activities.

In Supplementary Files S2–S4, we provide specifics of assigned EC, SCOP and GO annotations, respectively, for each member of created clusters. The first two columns in Figure 8 are just a snapshot of what kind of information is reported in these files. Closer examination of these assignments for members of each cluster shows that similar pockets that are clustered together by PDBspheres share similar functions.

Another important question is: Can we transfer binding affinity scores from one ligand binding site to another if the pockets and the ligand placements within the pockets are similar? Results from PDBspheres analysis suggest that pockets from PDBbind that share high structure similarity and have similar ligand placements (distances between the centroids of inserted ligands are no greater than 0.5 Å) show also similarities in reported protein–ligand binding affinities. In particular, for PDBbind entries with known K_{d} values, in Figure 9A we compare the K_{d} values of each pair of 1544 protein–ligand complexes when GDC is >95% and aligned ligand centroids are within 0.5 Å. The R^2 and Spearman values of 0.5 and 0.7, respectively, indicate the strength of the relation. Although reported scores are not very high, they can still suggest that with required similarity constraints the similar protein–ligand pairs tend to have similar K_{d} values. Similarly, in Figure 9B, the pockets with given K_{i} values and the same similarity constraints show the R^2 and Spearman values of 0.44 and 0.574, respectively, for 5137 evaluated protein–ligand pairs.

These similarities in binding affinities are even higher between pockets from different proteins when they bind the same ligand. The corresponding R^2 and Spearman scores for 194 pairs with K_{d} values are 0.5 and 0.738, and for 411 pairs with K_{i} values are 0.69 and 0.772, respectively. Even if we relax the similarity constraints by requiring a ligand centroid's distance cutoff of 1.0 Å and GDC pocket similarities as low as 90%, for pocket pairs that bind the same ligands, as shown in Figure 10A and B, for the K_{d} subset of 287 pairs the R^2 and Spearman values are 0.46 and 0.703, and for the K_{i} subset of 631 pairs the scores are 0.64 and 0.752, respectively.

Results from the PDBspheres clustering of the PDBbind dataset suggest that the structure similarity between pocket/ligand placements is a significant characteristic that can allow prediction of similar binding affinity values. In future work, we anticipate enhancing current measurements adding information about the specific atom location of protein residues interacting with the ligand, which may improve our predictions. Complete results from PDBspheres analysis of pairwise similarities in binding sites between proteins from PDBbind are provided in Supplementary File S5.

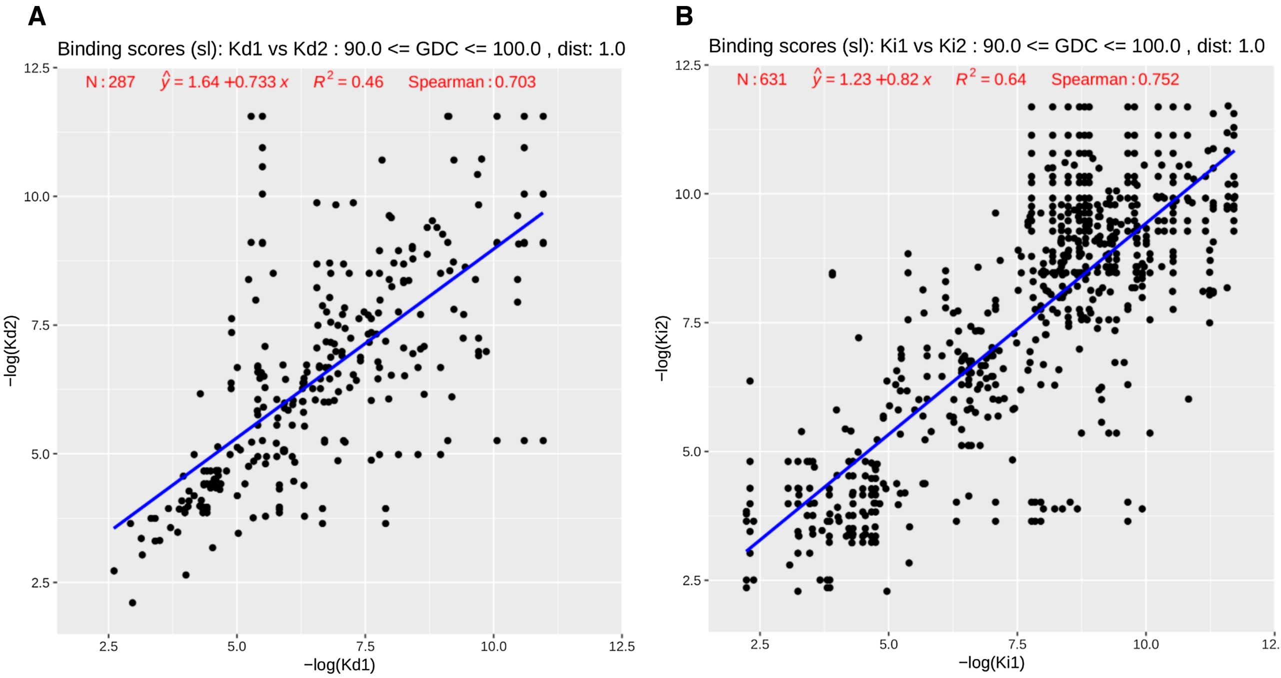

Figure 10. Scatter plots of (**A**) K_{d} values from 287 ‘same ligand’ pocket pairs and (**B**) K_{i} values from 631 ‘same ligand’ pocket pairs. Results shown in the plot were calculated for pairs satisfying slightly relaxed similarity constraints: pocket GDC similarities ≥90% and ligand centroid’s distance cutoff of 1.0 Å. Redundant pairs—self-comparisons and symmetry duplicates—are removed from calculations.

CONCLUSIONS

While developing PDBspheres, we focused on two goals: (i) binding pocket detection and (ii) identification of characteristics and scores to assess similarities between pockets to help further protein functional characterization and clustering.

In particular, with regard to binding pocket detection, we find that PDBspheres’ strictly structure-based approach can correctly predict binding site regions in protein structures known to be in a ‘holo’ (i.e. ligand-binding) conformation as well as in protein structures in an ‘apo’ (without a ligand present) conformation. While we are not directly comparing our method with other template-based binding site prediction methods, we can estimate that PDBspheres has very similar accuracy when assessed by MCC between predicted and observed binding residues. CASP experiments (CASP8–10) indicated that in comparison with other methods the template-based methods were performing on the top with reported average MCC scores slightly above 0.7. For example, the average scores for the best-performing template-based methods at CASP10 Firestar and SP-ALIGN were 0.715 and 0.707, respectively. Results from testing PDBspheres on LBSp dataset, reported in Table 1, show that the average MCC score for PDBspheres is at the similar level (∼0.71) when the closest to the targeted protein homologous template spheres are being removed from the library. As shown in Table 1, when the sequence identity drops, there is an immediate decline in the average MCC values from ∼0.8 (for 100% SeqID when the exact or very close match can be found in the library) to ∼0.7 (for 90% to 50% SeqID when possible best matches are being eliminated). Interestingly, in case of restricted libraries, the average MCC value seems to reach a steady level of ∼0.7, which agrees with results of evaluation of template-based methods in CASP8–10 experiments (22–24).

Since local regions in functionally similar proteins are remarkably conserved in their structural conformations, the PDBspheres method allows detection of similar binding sites even in proteins that share very low sequence similarity. Based on this observation and our tests on the LBSp benchmark dataset with restricted libraries, we can expect that structure template-based methods may successfully predict 96% of pocket locations and reach the accuracy level in predicted binding residues measured by the average MCC of ∼0.7 for proteins that have no close representation in used libraries.

With regard to characterizing and evaluating binding pocket similarities among proteins, we find that a high level of sequence similarity between different proteins is not essential to identify structurally similar binding sites and that proteins even significantly different by sequence may perform similar functions. In the structure-based detection of binding sites, the similarity assessed based on calculated structural alignment using C-alpha atom positions is sufficient, and the use of other residues (e.g. C-beta atoms or other points representing residue) in the similarity assessment does not yield better results. Structurally similar binding pockets having similar ligand placements allow inference of binding affinity from one pocket–ligand pair to another pocket–ligand pair. PDBspheres-based clustering of detected pockets and calculated structure similarities among pockets from different proteins provide information that can significantly help protein function annotation efforts.

DATA AVAILABILITY

All supplementary data, libraries and files with the PDBspheres system's installation and usage instructions are publicly available at https://github.com/LLNL/PDBspheres.

SUPPLEMENTARY DATA

Supplementary Data are available at NARGAB Online.

ACKNOWLEDGEMENTS

This work was performed under the auspices of the U.S. Department of Energy by Lawrence Livermore National Laboratory under Contract DE-AC52-07NA27344.

FUNDING

American Heart Association [CRADA TC02274 to F.C.L.]; Laboratory Directed Research and Development [LDRD 20-ERD-062 to J.E.A.]; DTRA [HDTRA1036045 to J.E.A.].
Conflict of interest statement. None declared.

REFERENCES

1. Kahraman,A., Morris,R.J., Laskowski,R.A., Favia,A.D. and Thornton,J.M. (2010) On the diversity of physicochemical environments experienced by identical ligands in binding pockets of unrelated proteins. *Proteins*, **78**, 1120–1136.
2. Gao,M. and Skolnick,J. (2013) A comprehensive survey of small-molecule binding pockets in proteins. *PLoS Comput. Biol.*, **9**, e1003302.
3. Degac,J., Winter,U. and Helms,V. (2015) Graph-based clustering of predicted ligand-binding pockets on protein surfaces. *J. Chem. Inf. Model.*, **55**, 1944–1952.
4. Konc,J. and Janezic,D. (2010) ProBiS algorithm for detection of structurally similar protein binding sites by local structural alignment. *Bioinformatics*, **26**, 1160–1168.
5. Glaser,F., Morris,R.J., Najmanovich,R.J., Laskowski,R.A. and Thornton,J.M. (2006) A method for localizing ligand binding pockets in protein structures. *Proteins*, **62**, 479–488.
6. Spitzer,R., Cleves,A.E. and Jain,A.N. (2011) Surface-based protein binding pocket similarity. *Proteins*, **79**, 2746–2763.
7. Ehrt,C., Brinkjost,T. and Koch,O. (2018) A benchmark driven guide to binding site comparison: an exhaustive evaluation using tailor-made data sets (ProSPECCTs). *PLoS Comput. Biol.*, **14**, e1006483.
8. Govindaraj,R.G. and Brylinski,M. (2018) Comparative assessment of strategies to identify similar ligand-binding pockets in proteins. *BMC Bioinformatics*, **19**, 91.
9. Kahraman,A., Morris,R.J., Laskowski,R.A. and Thornton,J.M. (2007) Shape variation in protein binding pockets and their ligands. *J. Mol. Biol.*, **368**, 283–301.
10. Hoffmann,B., Zaslavskiy,M., Vert,J.P. and Stoven,V. (2010) A new protein binding pocket similarity measure based on comparison of clouds of atoms in 3D: application to ligand prediction. *BMC Bioinformatics*, **11**, 99.
11. Dias,S., Simões,T., Fernandes,F., Martins,A.M., Ferreira,A, Jorge,J. and Gomes,A.J.P. (2019) CavBench: a benchmark for protein cavity detection methods. *PLoS One*, **14**, e0223596.
12. Jiménez,J., Doerr,S., Martínez-Rosell,G., Rose,A.S. and De Fabritiis,G. (2017) DeepSite: protein-binding site predictor using 3D-convolutional neural networks. *Bioinformatics*, **33**, 3036–3042.
13. Jones,D., Kim,H., Zhang,X., Zemla,A., Stevenson,G., Bennett,W.F., Kirshner,D., Wong,S.E., Lightstone,F.C. and Allen,J.E. (2021) Improved protein–ligand binding affinity prediction with structure-based deep fusion inference, *J. Chem. Inf. Model.*, **61**, 1583–1592.
14. Stepniewska-Dziubinska,M.M., Zielenkiewicz,P. and Siedlecki,P. (2020) Improving detection of protein–ligand binding sites with 3D segmentation. *Sci. Rep.*, **10**, 5035.
15. Stepniewska-Dziubinska,M.M., Zielenkiewicz,P. and Siedlecki,P. (2019) Detection of protein–ligand binding sites with 3D segmentation (v1). arXiv doi: https://arxiv.org/abs/1904.06517, 13 April 2019, preprint: not peer reviewed.
16. López,G., Valencia,A. and Tress,M.L. (2007) Firestar—prediction of functionally important residues using structural templates and alignment reliability. *Nucleic Acids Res.*, **35**, W573–W577.
17. Brylinski,M. and Skolnick,J. (2008) A threading-based method (FINDSITE) for ligand-binding site prediction and functional annotation. *Proc. Natl Acad. Sci. U.S.A.*, **105**, 129–134.
18. Capra,J.A., Laskowski,R.A., Thornton,J.M., Singh,M. and Funkhouser,T.A. (2009) Predicting protein ligand binding sites by combining evolutionary sequence conservation and 3D structure. *PLoS Comput. Biol.*, **5**, e1000585.
19. Laskowski,R.A. (1995) SURFNET: a program for visualizing molecular surfaces, cavities, and intermolecular interactions. *J. Mol. Graph.*, **13**, 323–308.
20. Dukka,B.K.C. (2013) Structure-based methods for computational protein functional site prediction. *Comput. Struct. Biotechnol. J.*, **8**, e201308005.
21. Powell,J., Mota,F., Steadman,D., Soudy,C., Miyauchi,J.T., Crosby,S., Jarvis,A., Reisinger,T., Winfield,N., Evans,G. *et al.* (2018) Small molecule neuropilin-1 antagonists combine antiangiogenic and antitumor activity with immune modulation through reduction of transforming growth factor beta (TGF beta) production in regulatory T-cells. *J. Med. Chem.*, **61**, 4135–4154.
22. López,G., Ezkurdia,I. and Tress,M.L. (2009) Assessment of ligand binding residue predictions in CASP8. *Proteins*, **77**, 138–146.
23. Schmidt,T., Haas,J., Cassarino,T.G. and Schwede,T. (2011) Assessment of ligand-binding residue predictions in CASP9. *Proteins*, **79**, 126–136.
24. Cassarino,T.G., Bordoli,L. and Schwede,T. (2014) Assessment of ligand binding site predictions in CASP10. *Proteins*, **82**, 154–163.
25. Clark,J.J., Orban,Z.J. and Carlson,H.A. (2020) Predicting binding sites from unbound versus bound protein structures. *Sci. Rep.*, **10**, 15856.
26. Clark,J.J., Benson,M.L., Smith,R.D. and Carlson,H.A. (2019) Inherent versus induced protein flexibility: comparisons within and between apo and holo structures. *PLoS Comput. Biol.*, **15**, e1006705.
27. Berman,H.M., Westbrook,J., Feng,Z., Gilliland,G., Bhat,T.N., Weissig,H., Shindyalov,I.N. and Bourne,P.E. (2000) The Protein Data Bank. *Nucleic Acids Res.*, **28**, 235–242.
28. Zemla,A. (2003) LGA: a method for finding 3D similarities in protein structures. *Nucleic Acids Res.*, **31**, 3370–3374.
29. Keedy,D.A., Williams,C.J., Headd,J.J., Arendall,W.B. 3rd, Chen,V.B., Kapral,G.J., Gillespie,R.A., Block,J.N., Zemla,A., Richardson,D.C. *et al.* (2009) The other 90% of the protein: assessment beyond the Calphas for CASP8 template-based and high-accuracy models. *Proteins*, **77**, 29–49.
30. Yoon,S., Ebert,J.C., Chung,E.Y., De Micheli,G. and Altman,R.B. (2007) Clustering protein environments for function prediction: finding PROSITE motifs in 3D. *BMC Bioinformatics*, **8**(Suppl. 4), S10.
31. Pearson,W.R. (2016) Finding protein and nucleotide similarities with FASTA. *Curr. Protoc. Bioinformatics*, **53**, 3.9.1–3.9.25.
32. Maggiora,G., Vogt,M., Stumpfe,D. and Bajorath,J. (2014) Molecular similarity in medicinal chemistry. *J. Med. Chem.*, **57**, 3186–3204.
33. Guterres,H., Park,S., Jiang,W. and Im,W. (2021) Ligand-binding-site refinement to generate reliable holo protein structure conformations from apo structures. *J. Chem. Inf. Model.*, **61**, 535–546.
34. Chen,K., Mizianty,M.J., Gao,J. and Kurgan,L. (2011) A critical comparative assessment of predictions of protein-binding sites for biologically relevant organic compounds. *Structure*, **19**, 613–621.
35. Kawabata,T. (2010) Detection of multiscale pockets on protein surfaces using mathematical morphology. *Proteins*, **78**, 1195–1211.
36. Huang,B. and Schroeder,M. (2006) LIGSITE^{csc}: predicting ligand binding sites using the Connolly surface and degree of conservation. *BMC Struct. Biol.*, **6**, 19.
37. Le Guilloux,V., Schmidtke,P. and Tuffery,P. (2009) Fpocket: an open-source platform for ligand pocket detection. *BMC Bioinformatics*, **10**, 168.

38. Tan,K.P., Varadarajan,R. and Madhusudhan,M.S. (2011) DEPTH: a web server to compute depth and predict small-molecule binding cavities in proteins. *Nucleic Acids Res.*, **39**, W242–W248.
39. Ravindranath,P.A. and Sanner,M.F. (2016) AutoSite: an automated approach for pseudo-ligands prediction—from ligand-binding sites identification to predicting key ligand atoms. *Bioinformatics*, **32**, 3142–3149.
40. Wang,R., Fang,X., Lu,Y. and Wang,S. (2004). The PDBbind database: collection of binding affinities for protein–ligand complexes with known three-dimensional structures. *J. Med. Chem.*, **47**, 2977–2980.